Mol Biotechnol (2012) 52:251–261
DOI 10.1007/s12033-011-9489-0

RESEARCH

# Expression and Functional Analysis of Two Osmotin (PR5) Isoforms with Differential Antifungal Activity from *Piper colubrinum*: Prediction of Structure–Function Relationship by Bioinformatics Approach

**Tomson Mani · K. C. Sivakumar · S. Manjula**

Published online: 30 December 2011


**Abstract** Osmotin, a pathogenesis-related antifungal protein, is relevant in induced plant immunity and belongs to the thaumatin-like group of proteins (TLPs). This article describes comparative structural and functional analysis of the two osmotin isoforms cloned from *Phytophthora*-resistant wild *Piper colubrinum*. The two isoforms differ mainly by an internal deletion of 50 amino acid residues which separates them into two size categories (16.4 kDa—*PcOSM1* and 21.5 kDa—*PcOSM2*) with p*I* values 5.6 and 8.3, respectively. Recombinant proteins were expressed in *E. coli* and antifungal activity assays of the purified proteins demonstrated significant inhibitory activity of the larger osmotin isoform (*PcOSM2*) on *Phytophthora capsici* and *Fusarium oxysporum*, and a markedly reduced antifungal potential of the smaller isoform (*PcOSM1*). Homology modelling of the proteins indicated structural alterations in their three-dimensional architecture. Tertiary structure of *PcOSM2* conformed to the known structure of osmotin, with domain I comprising of 12 $\beta$-sheets, an $\alpha$-helical domain II and a domain III composed of 2 $\beta$-sheets. *PcOSM1* (smaller isoform) exhibited a distorted, indistinguishable domain III and loss of 4 $\beta$-sheets in domain I. Interestingly, an interdomain acidic cleft between domains I and II, containing an optimally placed endoglucanase catalytic pair composed of Glu–Asp residues, which is characteristic of antifungal PR5 proteins, was present in both isoforms. It is well accepted that the presence of an acidic cleft correlates with antifungal activity due to the presence of endoglucanase catalytic property, and hence the present observation of significantly reduced antifungal capacity of *PcOSM1* despite the presence of a strong acidic cleft, is suggestive of the possible roles played by other structural features like domain I or/and III, in deciding the antifungal potential of osmotin.

**Keywords** Black pepper · *Phytophthora capsici* · Quick wilt · Defence elicitors · Homology modelling

**Electronic supplementary material** The online version of this article (doi:10.1007/s12033-011-9489-0) contains supplementary material, which is available to authorized users.

T. Mani · S. Manjula (✉)
Plant Molecular Biology Division, Rajiv Gandhi Centre for Biotechnology, Thycaud, Thiruvananthapuram 695014, Kerala, India
e-mail: smanjula@rgcb.res.in

T. Mani
e-mail: tomsonmani@gmail.com

*Present Address:*
T. Mani
Department of Botany, St. Berchmans College, Changanassery, Kerala, India

K. C. Sivakumar
Bioinformatics Division, Rajiv Gandhi Centre for Biotechnology, Thycaud, Thiruvananthapuram 695014, Kerala, India
e-mail: siva@rgcb.res.in

## Introduction

Plants defend themselves by deploying a plethora of defence-related molecules against the invading pathogens at each level of defence [1]. Plant pathogenesis-related (PR) proteins are such a group of effector molecules expressed under pathological conditions. These proteins are classified into different families based on functional features and serological relationships [2, 3]. PR 5 family proteins are a group of antimicrobial proteins with diverse functions in plants. Members of this family show similarity

to thaumatin, a sweet tasting protein found in the arils of the plant *Thaumatococcus danielli* and hence are also called thaumatin-like proteins (TLPs) [3]. Members include the well-known antifungal proteins zeamatin and osmotin which show prominent antifungal activity in vitro and in vivo [4–8]. Transgenic over expression of PR 5 proteins in plants has resulted in delay in onset of disease symptoms, indicating their potential as candidate genes for genetic engineering of plants [7, 9, 10]. Experiments on isolated yeast (*Saccharomyces cerevisiae*) spheroplasts and other fungal cells have predicted plasma membrane as the target of protein activity [6, 11–13] and membrane permeabilization as the possible method of action [4, 6, 12]. Studies on yeast cells have also shown that cell wall components like carbohydrates and proteins could regulate osmotin sensitivity, as the presence of phosphomannans-enhanced osmotin activity while other cell wall-related proteins like PIR2 and SSD1 caused osmotin resistance [11, 14, 15]. Recent studies indicate that osmotin shares structural similarity to adiponectin, an antidiabetic, and antiatherosclerotic protein hormone in mammals that conditions sensing of energy status, fatty acid oxidation, and glucose transport upon interaction with adiponectin receptors [16, 17]. Both osmotin and adiponectin have lectin-like domain structure and their comparative functional studies in yeast cells and C2C12 myocytes have shown a receptor-mediated mechanism of action [16, 17]. Thus, osmotin, due to its functional similarity to adiponectin, has recently been highlighted as an agonist molecule with therapeutic potential [17].

The accepted model of TLPs comprises a three domain structure stabilized by disulphide bridges [18–22]. A notable feature is the presence of an acidic cleft between domains I and II, which possesses amino acid residues acting as catalytic pair capable of glucan hydrolysis. This is cited as a structural feature required for antifungal activity of TLP as it has been shown that several TLPs can bind to $\beta$-1,3-glucans and many of them can hydrolyse polymeric glucan molecules which are common constituents of fungal cell walls [23–26]. However, the glucanase activity exhibited by the TLPs is by far very low when compared to that of glucanases belonging to PR-2 class [25, 26]. There are also reports of antifungal TLPs which are devoid of glucanase activity, which leads to the inference that additional structural features could be involved in determining the antifungal activity of TLP [20, 21, 26].

In our earlier work, we identified two osmotin isoforms from a defence gene-enriched cDNA subtracted library of *Phytophthora*-resistant wild pepper—*Piper colubrinum* and carried out a comparative sequence analysis of the two forms. Accordingly, the smaller form *PcOSM1*, of molecular weight 16.4 kDa (EU271754.1) shows an internal deletion of 50 amino acids [27]. The present report focuses on expression of the recombinant isoforms in *E. coli* and their antifungal functional validation on the plant fungal pathogens *Phytophthora capsici* (causative organism of foot rot disease of cultivated black pepper *Piper nigrum* [28]) and *Fusarium oxysporum.* Protein functional studies of *P. colubrinum* osmotin isoforms was further extended to structural prediction using bioinformatics tools, in an attempt to provide possible insight into the hitherto unidentified roles played by additional structural features of TLPs in determining protein functionality.

## Materials and Methods

### Plant Material and Treatments

Healthy plants of *P. colubrinum* link, maintained in the greenhouse of Rajiv Gandhi Centre for Biotechnology, Trivandrum, India were used for this study. To analyse the relative effect of abiotic stress inducing compounds and different signalling compounds on the expression of *P. colubrinum* osmotin isoforms, fully expanded leaves were sprayed with ethephon (1 mg/ml)/1 mM SA/1 mM MeJ solutions in water. The leaves were inoculated with virulent PDA grown cultures of *P. capsici* to study the relative expression of the isoforms under biotic stress. The abaxial sides of leaves were needle-pricked and mycelial discs were placed on the wound. Needle-pricked leaves free of mycelial discs were used to study the effect of wounding on the expression level of the genes and also served as control for pathogen inoculation study. The treatments were carried out for a period of 24 h and the plants were kept covered using plastic bags until sampling.

### Sequence Analysis

Homology searches were performed with BLAST to confirm sequence identity. The amino acid sequences of PR-5 proteins representing dicots and monocots were retrieved from NCBI Genbank and multiple sequence alignment was performed with *PcOSM1* and *PcOSM2* sequences using the online tool available at www.ebi.ac.uk and the programme GeneDoc (http://www.nrbsc.org/gfx/genedoc). The programmes Signal P (http://www.cbs.dtu.dk/services/SignalP/) and Target P (http://www.cbs.dtu.dk/services/TargetP/) were used to predict the cellular location of *P. colubrinum* osmotin isoforms.

### Expression Analysis of *P. colubrinum* Osmotin Isoforms

Real-time PCR analyses were carried out to determine comparative tissue-specific transcript abundance of the

**Table 1** Primers used for subcloning *P. colubrinum* osmotin isoforms into pET 32 a vector

| | |
|---|---|
| Forward primer | 5′-ATCCCATATGCATCATCACCATCACCATGCCAACTCCTAATAAGGAACAACTG-3′ |
| Reverse primer | 5′-CCATTAAGCTTTCATGGGCAGAAG-3′ |
| *Primers used for real-time PCR—PcOSM1* | |
| Forward primer | 5′-ACCGTCTGGGCCGCCGGCG-3′ |
| Reverse primer | 5′-GCTGTGCATTGGAGGACGCCG-3′ |
| *Primers used for real-time PCR—PcOSM2* | |
| Forward primer | 5′-CCTCAACGTCCCGGCAGGCACC-3′ |
| Reverse primer | 5′-CGCCGCAGTCGCCGGTCTGGCAAC-3′ |

osmotin isoforms and its accumulation in response to defence elicitors like SA, MeJ, ethylene and the pathogen *P. capsici*. Total RNA was isolated like from leaf, stem, root, spike and elicitor-treated leaves of *P. colubrinum*. Approximately, 1 μg of DNase (Sigma, St. Louis) treated RNA was used to prepare cDNA using MMLV-RT following manufacturer's protocol (Promega, Madison, WI). Gene specific primers (Table 1) amplifying a 100 bp product were used for quantitative real-time PCR. The reaction was set up in a final volume of 20 μl containing 10 μl SYBR green PCR reagent (Applied Biosystems, CA), 1 μl of diluted cDNA and 300 nM each of the designed primers and the conditions were 50°C for 2 min initially followed by 95°C for 10 min and 40 cycles of 95°C for 15 s and 60°C for 1 min in a real-time PCR machine (ABI 7500, Applied Biosystems, CA). Three replicates each from two biological samples were used for each analysis. The house keeping gene $\beta$-actin cloned from *P. colubrinum* was used for normalisation and the relative expression level of the genes was determined by the comparative $C_t$ method using the SDS software (Applied Biosystems, CA).

## Statistical Analysis

Real-time analysis for transcript abundance of osmotin isoforms in each tissue as well as in response to each defence elicitor was performed in triplicate and each experiment was repeated twice ($n = 6$). Resultant mean values were analysed by Student's '*t*' test and values were considered significant at $P < 0.05$.

## Prokaryotic Expression and In Vitro Antifungal Assay of Osmotin Isoforms

Osmotin isoforms cloned from *P. colubrinum* were expressed in recombinant *E. coli* BL21(DE3) pLyS (Invitrogen, Carlsbad) or JM109(DE3) pLyS (Promega, Madison, WI) using the expression vector pET 32a (Novagen, USA). The coding sequence for the mature protein of the isoforms (*PcOSM1* and *PcOSM2*) was amplified using gene specific primers with sequences for histidine tag and restriction enzyme sites (Table 1). The amplicons were cloned into T/A cloning vector pGEMT—Easy (Promega, Madison, WI) and subcloned to pET 32 a (+) vector (Novagen, USA) at *Nde* I and *Hin*d III sites. Recombinant constructs were confirmed by sequencing in an automated sequencer (3730 DNA analyser, Applied Biosystems, CA) using T7 promoter primer and introduced into the expression host. The recombinant protein was induced using 0.8–1.0 mM IPTG (Gibco BRL, CA). Expressed protein was purified by nickel affinity chromatography under denaturing conditions and eluted fractions were pooled and dialysed against 20 mM Tris HCl (pH 7.2) as described by Hu and Reddy [29]. Dialysed protein was concentrated (Amicon concentrators, Millipore) and used for in vitro antifungal assay after quantification by Bradford method [30]. The total bacterial protein from each sample was separated on 12% SDS-PAGE and transferred to nitrocellulose membrane (Hybond C, Amersham) for Western blot analysis using Mini Trans-Blot Electrophoretic Transfer cell (Biorad, CA). Recombinant proteins were probed with anti-his tag antibody (Sigma, MO). For in vitro antifungal assay, spores of *P. capsici* ($1 \times 10^3$/100 μl) or conidia of *F. oxysporum* ($1 \times 10^3$/100 μl) taken in a microplate in triplicate was incubated with different concentrations of purified recombinant protein for 48 h. Optical density of fungal growth in each well was measured at 595 nm to check growth inhibitory activity of the protein [31, 32].

## Molecular Modelling of *PcOSM1* and *PcOSM2*

The amino acid sequences of *PcOSM1* and *PcOSM2* were first subjected to PSI-BLAST [33] with three iterations for finding homologous template. Consequently, the refined crystal structure of antifungal banana fruit TLP at resolution 1.7 Å from the Brookhaven Protein Data Bank (PDB entry 1Z3Q) was retrieved and used as the template. Homology modelling was performed using the programme Modeller9v2 [34]. The three-dimensional structure prediction was carried out by alignment of target sequence with template structure. Models were built solely based on heavy atoms, and are likely to be a first approximation of

the three-dimensional structure of antifungal banana fruit TLP. Modeller has an advantage over other such programs in allowing experimentally derived distance restraints to be used in conjunction with restraints from the homologous structures in deriving the model. A total of 50 models were produced and refined within Modeller. Conformational clustering of the final models, and identification of structures 'representative' of the ensemble of models, were performed using the program NMRCLUST [35]. Backbone conformation of the refined structure was evaluated by comparing the *Z* score of *PcOSM1* and *PcOSM2* and the template estimated using Prosa2003 [36]. Deviation of the modelled structure from the template was assessed by computing root-mean-square deviation (RMSD) values for positional differences between equivalent atoms following the superposition of Cα traces and backbone atoms of the model onto the template.

### Docking of (1, 3)-β-D Glucan with *PcOSM1* and *PcOSM2*

Docking of (1,3)-β-D glucan with *PcOSM1/2* was performed with AUTODOCK4.1 [37]. The procedure involved creation of a 8 Å grid centred on acidic cleft. Ligand charges were computed using the Gasteiger method. The binding affinity of (1,3)-β-D glucan to the acidic cleft of *PcOSM1/2* was studied using simulated annealing procedure of Accelrys Discovery Studio 2.0. Calculations were performed using the CHARMm Force-Fields PARM22 and the polysaccharide-specific CHEAT95 [38], and implemented in Discovery Studio. The simulation was performed for 500 ps with a time step of 0.001 and the temperature set to 300 K. The production type was set to NPT ensemble (constant temperature and pressure dynamics) with a radius of nonbonded interaction of 14.0 Å [39]. All simulation experiments were carried out using a DELL PowerEdge T300 Workstation with Quad Dual Intel Xeon 3.2 GHz processors.

## Results

### Sequence Analysis

*Piper colubrinum* osmotin isoforms share significant homology with corresponding sequences from other sources and show conserved residues of PR5 family members (Fig. 1). *PcOSM1* and TLPs from monocots like *Oryza sativa* var. *japonica* and *Secale cereale* [40] differ from other plant members in having an internal deletion of amino acid residues. In monocots, the deletion is present near the C-terminal of the sequence, which differs from

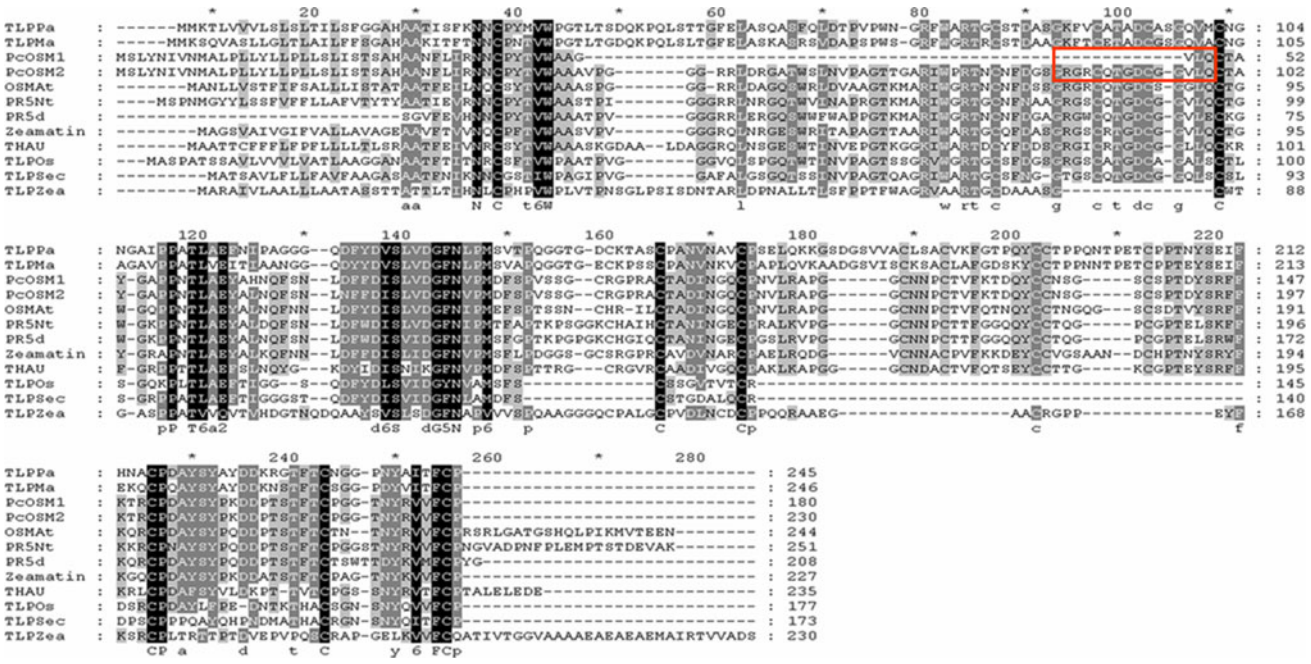

**Fig. 1** Sequence analysis. Multiple sequence alignment of amino acid sequences of *Piper colubrinum* osmotins (*PcOSM1*, *PcOSM2*) with TLPs from different taxa viz. *Prunus avium* (TLPPa, AAB38064), *Malus domestica* (TLPMa, CAC10270), *Arabidopsis thaliana* (OSMAt, AA61411), PR5 from *Nicotiana tabacum* (PR5Nt,CAA64620), PR-5d from tobacco [19], zeamatin (EU725369.1), thaumatin (THAU, AAA93095) *Oryza sativa* var. *japonica* (TLPOs, CAA48278.1), *Secale cereale* (TLPsec) [40] and *Zea mays* (NP_001147009.1). The *red rectangle* indicates the position of thaumatin signature sequence in *PcOSM2* (GRGRCQTGDCGGVLQ) which is truncated to four residues (GVLQ) in *PcOSM1* (Color figure online)

*PcOSM1* which possesses a deletion proximal to N-terminus. Multiple alignments of the sequences reveal characteristic conserved residues of TLP in *P. colubrinum* osmotins. It is, however, noteworthy that while *PcOSM2* retains the thaumatin signature sequence; it is partial in *PcOSM1* (Fig. 1). An N-terminal signal peptide is predicted in both isoforms and their secretory nature is predicted by *TARGET P*. The p*I* values of the two isoforms suggest that *PcOSM1* is an acidic protein (p*I* 5.6) and *PcOSM2* is a basic protein (p*I* 8.3).

## Expression Analysis of *P. colubrinum* Osmotin Isoforms

Real-time PCR analysis of transcript abundance (Fig. 2a) indicates that both *PcOSM1*and *PcOSM2* have the highest expression level in inflorescence (spike). The expression levels of the two transcripts were comparable in leaf and root. The abundance of *PcOSM1* transcript was greater than that of *PcOSM2* in inflorescence. On the other hand, *PcOSM2* transcript was more highly expressed than *PcOSM1* in stem. It is therefore evident from real-time PCR analyses that transcript levels of the two *P. colubrinum* osmotin isoforms show significant differences in tissue-specific expression.

*Piper colubrinum* osmotin isoforms show varied levels of expression in response to stress signals and pathogen. Figure 2b summarises the gene expression levels in biotic or abiotic elicitor-treated *P. colubrinum* leaves. Among the elicitors, ethylene favoured the highest accumulation of both *PcOSM1* and *PcOSM2* transcripts. *PcOSM2* was more abundant than *PcOSM1* in MeJ, *P. capsici* and salicylic acid-treated leaves. *PcOSM1* showed higher transcript accumulation in wounded leaves compared to *PcOSM2*. It is therefore evident from real-time PCR analyses that relative levels of the two *P. colubrinum* osmotin transcripts in leaves differ in response to various elicitor treatments.

## Prokaryotic Expression and In Vitro Antifungal Assay of *P. colubrinum* Osmotin Isoforms

The isoforms were expressed in *E. coli* under IPTG induction. Figure 3 shows the gel analysis of purified pET-*PcOSM1* and pET-*PcOSM2* recombinant proteins. Both the recombinant forms were detected positive in Western blot analysis using anti-his tag antibody (Fig. 3c). The fungal inhibitory activity of purified recombinant proteins is

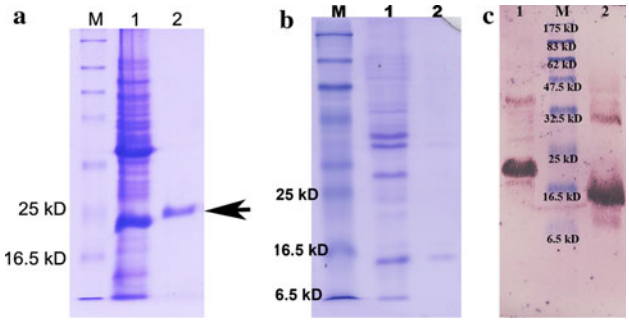


**Fig. 3** Prokaryotic expression of *P. colubrinum* osmotin isoforms. **a** SDS-PAGE (12%) analysis of recombinant *PcOSM1* (pET-*PcOSM1*) expression in *E. coli*. M—broad range protein marker (NEB, USA), 1—total protein of IPTG (0.8 mM)-induced bacteria harbouring recombinant construct, pET-*PcOSM1*, 2—purified recombinant *PcOSM1* protein. **b** SDS-PAGE analysis of recombinant *PcOSM2* (pET-*PcOSM2*) expression in *E. coli*. M—broad range protein marker (NEB,USA), 1—total protein of IPTG (0.8 mM)-induced bacteria harbouring recombinant construct, pET-*PcOSM2*, 2—purified recombinant *PcOSM2* protein. **c** Western blot of histidine tagged recombinant *P. colubrinum* osmotin isoforms. The recombinant protein samples are probed with anti-His tag antibody and developed by alkaline phosphatase reaction. 1—pET-*PcOSM2*, M—broad range protein marker, 2—pET-*PcOSM1*

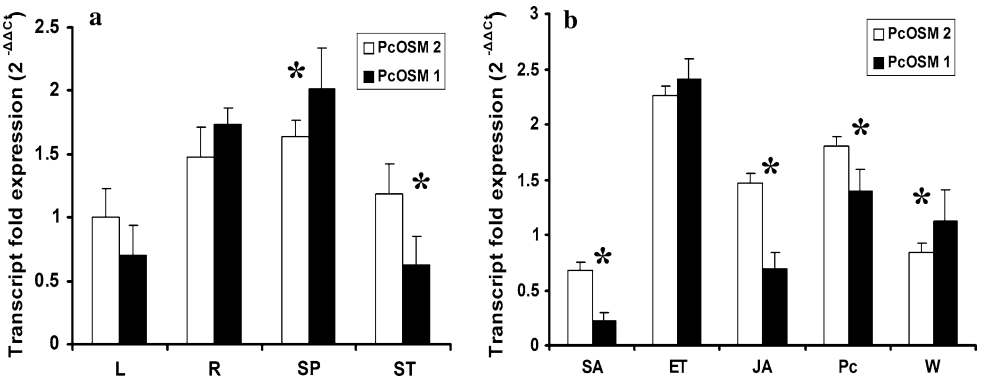


**Fig. 2** qRT-PCR analysis of *P. colubrinum* osmotin isoforms. **a** Tissue-specific expression analysis of *PcOSM1* and *PcOSM2*. L—leaf, R—root, St—stem and Sp—spike. **b** Expression analysis of *PcOSM1* and *PcOSM2* in leaves treated with various defence elicitors. SA—salicylic acid, ET—ethylene, JA—jasmonic acid, Pc—*Phytophthora capsici* and W—Wounding. *Represents significance at $P < 0.05$; $n = 6$. *Y*-axis represents relative quantification values or fold expression change given by the Eq. $2^{-\Delta\Delta Ct}$

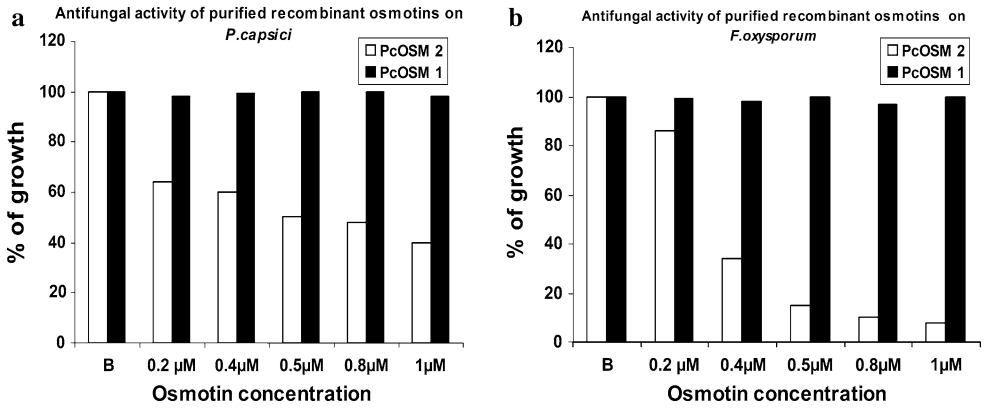


**Fig. 4** Antifungal activity of purified recombinant *P. colubrinum* osmotin isoforms. Effect of purified recombinant osmotins on germination and growth of *Phytophthora capsici* spore suspension (**a**) and *Fusarium oxysporum* conidial suspension (**b**). The experiment was repeated three times with triplicate samples which gave similar results. Shown are the results obtained from one experiment. Growth in each sample is expressed relative to growth in buffer-treated control and is the average of triplicate samples. Lanes 1—buffer control, 2–5—increasing concentrations of protein; 2—0.2 µM, 3—0.4 µM, 4—0.5 µM, 5—0.8 µM, 6—1 µM

shown in Fig. 4. Results show a significant difference in antifungal activity of the recombinant proteins. The larger form (*PcOSM2*) of *P. colubrinum* osmotin exhibits significant inhibitory activity against *P. capsici* and *F. oxysporum* (Fig. 4a, b).

## Homology Modelling and Docking Studies

Homology models of *PcOSM1* and *PcOSM2* are shown in Fig. 5. *PcOSM2* has the typical structure of TLPs with three distinct domains (I, II and III) but *PcOSM1* shows significant deviation from the TLP structure. In the *PcOSM1* model, domain I and II can be identified but the domain III is indistinguishable. Domain I of *PcOSM1* has six $\beta$-sheets (10 in *PcOSM2*), but domain II containing $\alpha$-helices are similar in both forms (Figs. 5, 6). The extent of structural deviation/alteration found in *PcOSM1*, from the typical TLP molecular structure can be inferred from Fig. 6. The loss of $\beta$-sheets in *PcOSM1* causes a marked alteration in the surface of the protein. Homology models also show that the proteins have an overall globular architecture with a cleft region formed between domains I and II (Fig. 7). In both forms, the cleft region formed is acidic in nature. Residues found in and around the acidic cleft in *PcOSM1* are 24Y, 25G, 27P, 29N, 31L, 33E, 44F, 46D, 48S, 50V, 51D, 92N, 94C, 95T, 98K, 102Y, 103C, 104C, 105N, 126Y, 128Y, 129P, 130K, 131D, 136T and in *PcOSM2* the residues are 41G, 43R, 74Y, 75G, 77P, 79N, 81L, 83E, 96D, 98S, 100V, 101D, 142N, 114C, 145T, 148K, 152Y, 153C, 154C, 155N, 176Y, 178Y, 179P, 180K, 181D, 186T. Among these, negative charge contributing residues are 33E, 46D, 51D, 131D in *PcOSM1* and 83E, 96D, 101D, and 181D in *PcOSM2*. The positions of the residues are relatively the same in the sequence as well as in the protein model of isoforms. 33E−51D residues in *PcOSM1* and 83E−101D residues in *PcOSM2* are situated in the cleft and extend across the cleft region (Fig. 5c, d). These residue pairs are most likely catalytic pairs for endoglucanase action as their distance and the position suit the definition of a catalytic pair. The distances calculated between the members of the pairs are 5.28 Å in *PcOSM2* and 6.47 Å in *PcOSM1* (Fig. 5c, d).

Docking experiments revealed residues that are able to interact by hydrogen bonding with glucan molecule (Fig. 8). In *PcOSM1*, the residues are 24Y, 25G, 26A, 27P, 31L, 33E, 35A, 50V, 51D, 86A, 91N, 94C, 95T, 96V, 98K, 103C, 104C. In *PcOSM2*, the residues are 41G, 42A, 43R, 63G, 64D, 74Y, 76A, 77P, 78P, 81L, 83E, 100V, 101D, 134L, 136A, 141N, 144C, 145T, 146V, 148K, 179P. The interaction energies of the molecules are −287.3 kcal-mol$^{-1}$ for *PcOSM1* and −253.93 kcalmol$^{-1}$ for *PcOSM2*. The homology modelling and docking studies reveal the presence of catalytic pairs and the possibility of involvement of the two osmotin isoforms in the cleavage of carbohydrate molecules like glucans.

## Discussion

Transcript analysis of *P. colubrinum* osmotin isoforms shows a general over expression against various biotic and abiotic stimuli. It is evident that transcripts of smaller isoform, *PcOSM1* show high expression level similar to *PcOSM2* in response to pathogen, wounding, jasmonic acid and ethylene. This suggests a role for smaller forms of TLPs in plant–pathogen or plant–environment interaction. These smaller proteins may not have a direct inhibitory activity on the pathogen as evidenced by the absence of antifungal potential in vitro, but their possible indirect role

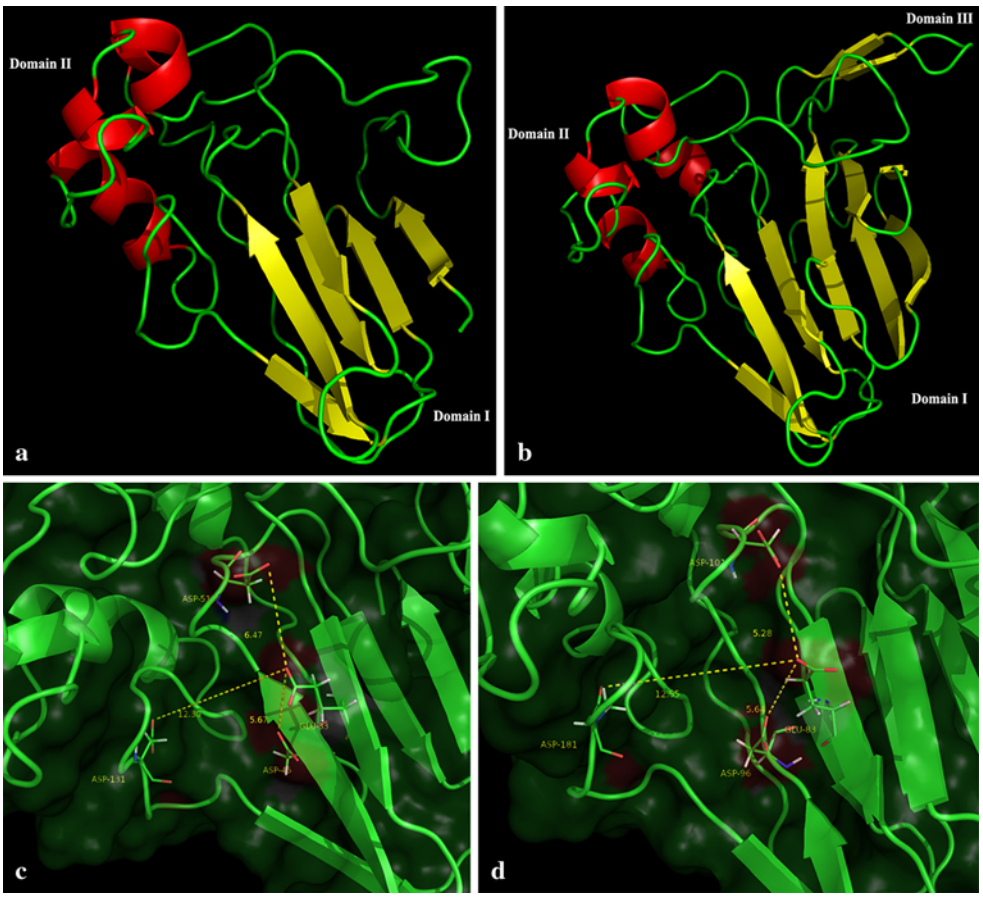


**Fig. 5** Homology models of TLPs. **a** Homology model of *PcOSM1*. Model shows the protein consisting of six $\beta$-sheets and four $\alpha$-helices connected by various loops. **b** Homology model of *PcOSM2*. Model shows the protein comprising of 12 $\beta$-sheets and four $\alpha$-helices. Models show differences in secondary structures. One common feature is that the proteins are cysteine rich and stabilized by disulphide bonds. *PcOSM2* shows the typical thaumatin-like structure with three distinct domains, whereas *PcOSM1* presents a distorted domain III. **c**, **d** shows the average distance between the acidic residues found in the cleft region of *P. colubrinum* osmotin isoforms. **c**, **d** Shows the catalytic pairs of *PcOSM1* and *PcOSM2* separated by 6.47 and 5.28 Å, respectively

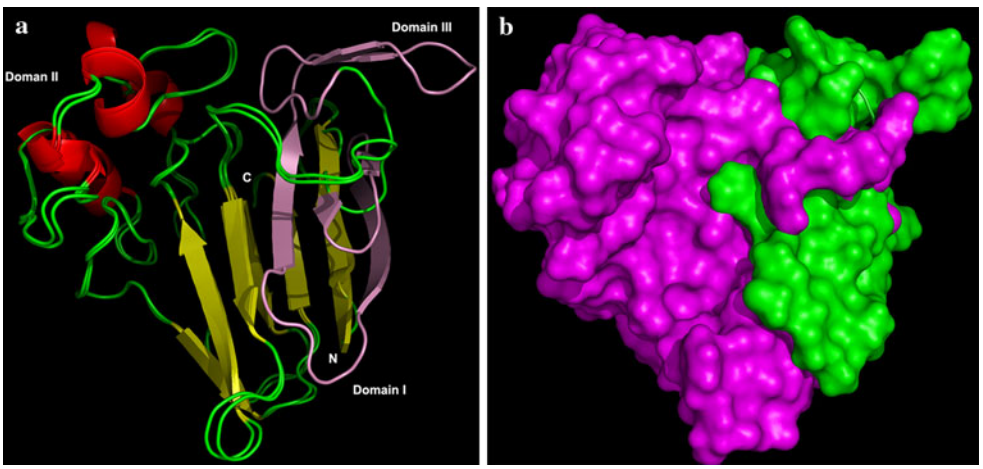


**Fig. 6** Secondary structure formed by the 'deletion' residues. **a** Shows the overlapped image of the 'ribbon models' of osmotin isoforms. The portion coloured in *pink* is lacking in smaller osmotin isoform (*PcOSM1*). **b** Shows the extent of shift in the molecular surface of the protein caused by deletion. *Green* coloured portion in this figure corresponds to the internal deletion found in *PcOSM1* (Color figure online)

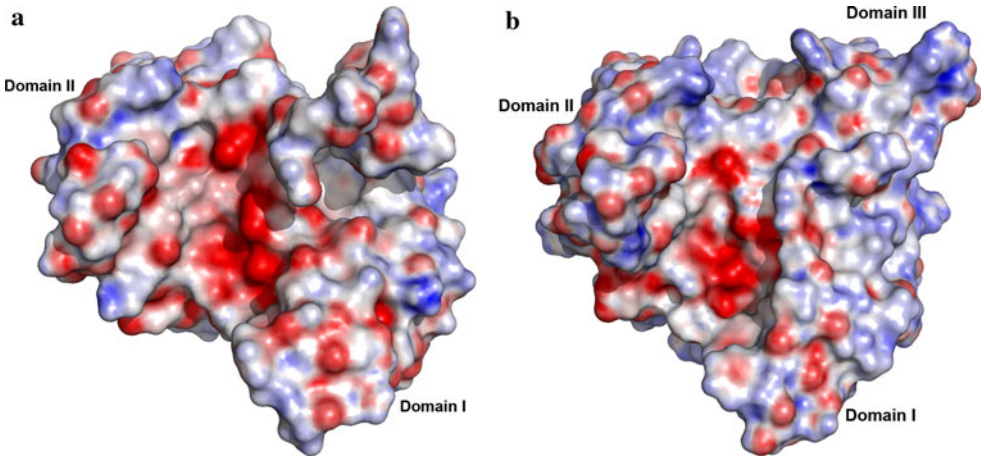


**Fig. 7** Molecular surface architecture of *P. colubrinum* osmotin isoforms. Distribution of charges on the surface of the molecule is shown as *red* (acidic) and *blue* (basic). **a** Shows the *PcOSM1* protein model harbouring a prominent acidic cleft between domains I and II similar to that found in *PcOSM2* model (**b**) (Color figure online)

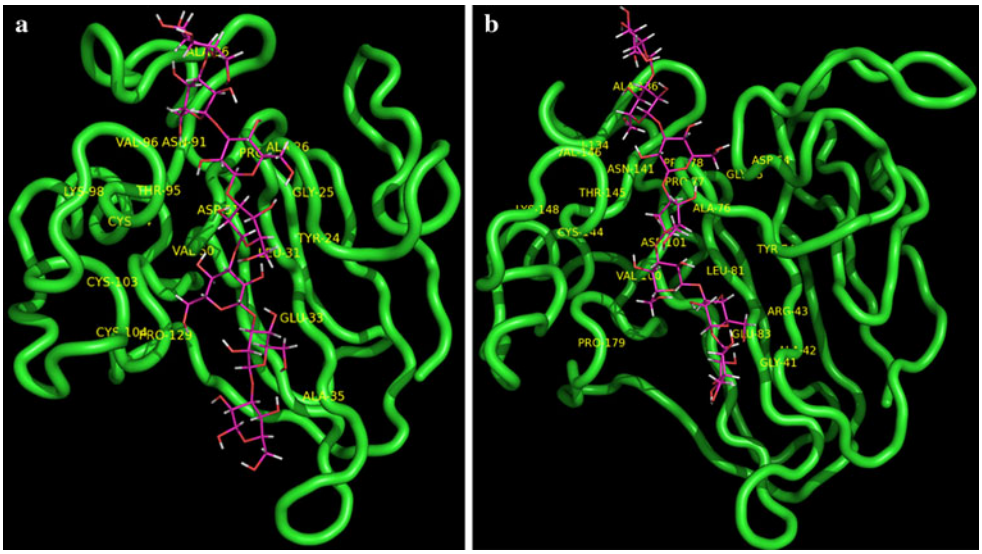


**Fig. 8** Docking experiment. Figure shows the interaction between *P. colubrinum* osmotin isoforms with (1, 3)-$\beta$-D-glucans in the cleft region. Interacting residues are labelled. **a** Shows the interactions in *PcOSM1*; **b** shows the interacting residues in *PcOSM2*

in impeding pathogen progress in plants cannot be ruled out.

The deduced amino acid sequences of *PcOSM1* and *2* are nearly identical except at the site of deletion [27]. The functional difference between the two osmotin isoforms in this study can possibly be attributed to the internal deletion of 50 amino acids in the smaller form. The internal deletion separates them into two size categories. Both forms of the protein possess an N-terminal signal peptide sequence indicating their extracellular location [27]. Structural information obtained from earlier models of antifungal TLPs—zeamatin, thaumatin, PR-5d, Osmotin and NP24-I provide a general model of TLPs having three distinct domains stabilized by disulphide bonds. An inter-domain acidic cleft has often been highlighted as a structural feature which is able to bind or hydrolyse $\beta$-1, 3-glucans, the constituents of fungal cell walls [19, 21, 25, 26]. In the homology models of *P. colubrinum* osmotin isoforms, an acidic cleft is recognised between domains I and II. The most striking feature of *PcOSM1* was the deletion of amino acid residues in the sequences and the distortion of domain III and four $\beta$-sheets in its domain I. Though the deletion caused distortion in the overall structure of *PcOSM1*, it is interesting to note that it has retained an inter-domain acidic cleft containing glucan-interacting residues. A closer analysis of the cleft region of osmotin isoforms shows that the major residues in the cleft are intact, including optimally placed catalytic pair, enabling them to retain glucan hydrolytic property. *PcOSM2* possesses a catalytic pair comprising 83E and 101D residues with a distance of 5.28 Å between them. In *PcOSM1*, the distance between the carboxylic oxygen atoms of the catalytic pair 33E and 51D is 6.47 Å. This data suggests that the glucan hydrolysing catalytic pair residues are at agreeable distance to

effect a glucan hydrolysis action [21, 26] suggestive of a glucan-catalytic function for both forms.

In spite of the presence of the structural features necessary for antifungal action, *PcOSM1* does not show any detectable inhibitory activity on the fungal species studied (*P. capsici*, *F. oxysporum*), compared to *PcOSM2*, which exhibits a strong antifungal potential. This observation reinforces earlier findings that the presence of acidic cleft alone may not be sufficient for the antifungal activity of TLPs, as the glucanase activity of TLP members to cause an inhibitory action against fungi is much lower compared to that shown by members of PR-2 family [21, 26].

It is possible that the structural alteration brought about by the internal deletion of amino acid residues in *PcOSM1* results in the marked difference in fungal inhibitory activity between the two isoforms, as even a subtle change in structure can bring about significant difference in protein action. Comparison with *PcOSM2* shows that the deletion residues comprise of six $\beta$-strands, four of which are constituents of domain I and the two remaining $\beta$-strands constitute a distinct domain III in *PcOSM2*. The deletion also causes a shift in the surface charge potential which probably determines the interaction of *PcOSM1* with other membrane-associated structures, a feature thought to be essential for antifungal activity of proteins [41–43].

Adiponectin is a protein hormone produced and secreted by fat cells (adipocytes), involved in the regulation of metabolism of lipids and glucose in mammals [16]. It was shown earlier in yeast that osmotin (24 kDa protein from *Nicotiana tabacum*) binds to a receptor which is a homologue of mammalian adiponectin receptor. It also shares functional similarity with adiponectin in triggering an AMP kinase pathway in C2C12 myocytes [16, 17]. In this study, both the osmotin isoforms are predicted as globular proteins and domains I and III of osmotin may significantly contribute to the similarity to adiponectin molecule. In the light of a previous observation that the action of TLPs could resemble K1 Killer toxin of yeast which has distinct binding and effector domains [44, 45], it is reasonable to infer from this study that the deleted residues in *PcOSM1* constitute or form a part of an effector domain which is responsible for the architectural similarity to the globular adiponectin molecule. The present comparative structural study of osmotin isoforms from *P. colubrinum* has identified putative structural features that could determine its activity. Analysis of these natural variants of the TLP family will provide additional insights into the evolutionary trend operating in the family where the different members are functionally optimised for diverse roles including defence. Though the osmotin isoforms in *P. colubrinum* differ in their inhibitory capacity on phytopathogenic fungi, the possibility of one form facilitating the action of the other, thus effecting a synergestic inhibitory activity on the fungal pathogen cannot be ruled out. This study warrants further in planta functional analysis of the isoforms which will rule out the possibility of protein misfolding associated with bacterial expression system, a point to be considered before establishing their functional divergence.

In conclusion, osmotin isoforms identified in *P. colubrinum* differ significantly in their antifungal activity. Despite the presence of a prominent acidic cleft, the smaller form of the protein is unable to exhibit detectable antifungal activity. Structural analysis showed that the internal deletion of *PcOSMI* caused significant structural alteration involving the loss of a proper domain III and four $\beta$-sheets from domain I. It brought changes in the surface charge potential of the protein as well. The absence of antifungal potential could be attributed to the loss of structural features caused by internal deletion highlighting the importance of domain III and domain I besides the presence of an acidic cleft in determining the antifungal activity of osmotins.

**Acknowledgments** Authors would like to thank Dr. N. Anith, Kerala Agricultural University, Vellayani, Trivandrum for the fungal strains. T.M. would like to acknowledge Council for Scientific and Industrial Research, New Delhi, Government of India, for CSIR-Junior Research Fellowship, and MS gratefully acknowledges the Department of Biotechnology, Government of India, for financial support in the form of research grant.

## References

1. Agrios, G. N. (2005). *Plant pathology*. Burlington: Elsevier Academic press.
2. Van Loon, L. C., Pierpoint, W. S., Boller, T., & Conejero, V. (1994). Recommendations for naming plant pathogenesis-related proteins. *Plant Molecular Biology Reporter, 12*, 245–264.
3. Velazhahan, R., Datta, S. K., & Muthukrishnan, S. (1999). The PR-5 family: Thaumatin-like proteins in plants. In S. K. Datta & S. Muthukrishnan (Eds.), *Pathogenesis-related proteins in plants* (pp. 107–129). Boca Raton: CRC press.
4. Roberts, W. K., & Selitrennikoff, C. P. (1990). Zeamatin, an antifungal protein from maize with membrane permeabilizing activity. *Journal of General Microbiology, 136*, 1771–1778.
5. Woloshuk, C. P., Meulenhoff, J. S., Sela-Buurlage, M., van den Elzen, P. J. M., & Cornelissen, B. J. C. (1991). Pathogen-induced proteins with inhibitory activity toward *Phytophthora infestans*. *Plant Cell, 3*, 619–628.
6. Abad, L. R., D'Urzo, M. P., Liu, D., Narasimhan, M. L., Reuveni, M., Zhu, J. K., et al. (1996). Antifungal activity of tobacco osmotin has specificity and involves plasma membrane permeabilisation. *Plant Science, 118*, 11–23.
7. Liu, D., Rhodes, D., D'Urzo, M. P., Xu, Y., Narasimhan, M. L., Hasegawa, P. M., et al. (1996). In vivo and in vitro activity of truncated osmotin that is secreted into the extracellular matrix. *Plant Science, 121*, 123–131.
8. Jami, S. K., Anuradha, T. S., Guruprasad, L., & Kirti, P. B. (2007). Molecular, biochemical and structural characterization of

osmotin-like protein from black nightshade (*Solanum nigrum*). *Journal of Plant Physiology, 164*, 238–252.
9. Liu, D., Raghothama, K. G., Hasegawa, P. M., & Bressan, R. A. (1994). Osmotin over expression in potato delays development of disease symptoms. *Proceedings of the National Academy of Science of the United States of America, 91*, 1888–1892.
10. Datta, K., Velazhahan, R., Oliva, N., Ona, I., Mew, T., & Khush, G. S. (1999). Over-expression of the cloned rice thaumatinlike protein (PR-5) gene in transgenic rice plants enhances environmently friendly resistance to Rhizoctonia solani causing sheath blight disease. *Theoretical and Applied Genetics, 98*, 1138–1145.
11. Yun, D. J., Zhao, Y., Pardo, J. M., Narasimhan, M. L., Damsz, B., & Lee, H. (1997). Stress proteins on the yeast cell surface determine resistance to osmotin, a plant antifungal protein. *Proceedings of the National Academy of Science of the United States of America, 94*, 7082–7087.
12. Anžlovar, S., Dalla Serra, M., Dermastia, M., & Menestrina, G. (1998). Membrane permeabilizing activity of pathogenesis-related protein linusitin from flax seed. *Molecular Plant-Microbe Interactions, 7*, 610–617.
13. Anžlovar, S., & Dermastia, M. (2003). The comparative analysis of osmotins and osmotin-like PR-5 proteins. *Plant Biology, 5*, 116–124.
14. Ibeas, J. I., Lee, H., Damsz, B., Prasad, D. T., Pardo, J. M., Hasegawa, P. M., et al. (2000). Fungal cell wall phosphomannans facilitate the toxic activity of a plant PR-5 protein. *Plant Journal, 23*, 375–383.
15. Narasimhan, M. L., Lee, H., Damsz, B., Singh, N. K., Ibeas, J. L., Mat-sumoto, T. K., et al. (2003). Overexpression of a cell wall glycoprotein in *Fusarium oxysporum* increases virulence and resistance to a plant PR-5 protein. *Plant Journal, 36*, 390–400.
16. Kadowaki, T., & Yamauchi, T. (2005). Adiponectin and adiponectin receptors. *Endocrine Reviews, 26*, 439–451.
17. Narasimhan, M. L., Coca, M. A., Jin, J., Yamauchi, T., Ito, Y., Kadowaki, T., et al. (2005). Osmotin is a homolog of mammalian adiponectin and controls apoptosis in yeast through a homolog of mammalian adiponectin receptor. *Molecular Cell, 17*, 171–180.
18. Batalia, M. A., Monzingo, A. F., Ernst, S., & Robertus, J. D. (1996). The crystal structure of the antifungal protein zeamatin, a member of the thaumatin-like, PR-5 protein family. *Nature Structural Biology, 3*, 19–23.
19. Koiwa, H., Kato, H., Nakatsu, T., Oda, J., Yamada, Y., & Sato, F. (1999). Crystal structure of tobacco PR-5d protein at 1.8 Å resolution reveals a conserved acidic cleft structure in antifungal thaumatin-like proteins. *Journal of Molecular Biology, 286*, 1137–1145.
20. Min, K., Ha, S. C., Hasegawa, P. M., Bressan, R. A., Yun, D., & Kim, K. K. (2004). Crystal structure of osmotin, a plant antifungal protein. *Proteins: Structure, Function, and Bioinformatics, 54*, 170–173.
21. Leone, P., Menu-Bouaouiche, L., Peumans, W. J., Payan, F., Barre, A., Roussel, A., et al. (2006). Resolution of the structure of the allergenic and antifungal banana fruit thaumatin like protein at 1.7-A°. *Biochimie, 88*, 45–52.
22. Ghosh, R., & Chakrabarti, C. (2008). Crystal structure analysis of NP24-I: A thaumatin-like protein. *Planta, 228*, 883–890.
23. Trudel, J., Grenier, J., Potvin, C., & Asselin, A. (1998). Several thaumatin-like proteins bind to $\beta$-1, 3-glucans. *Plant Physiology, 118*, 1431–1438.
24. Grenier, J., Potvin, C., Trudel, J., & Asselin, A. (1999). Some thaumatin-like proteins hydrolyse polymeric $\beta$-1, 3-glucans. *Plant Journal, 19*, 473–480.
25. Osmond, R. I., Hrmova, M., Fontaine, F., Imberty, A., & Fincher, G. B. (2001). Binding interactions between barley thaumatin-like proteins and (1, 3)-$\beta$-D-glucans. Kinetics, specificity, structural analysis and biological implications. *European Journal of Biochemistry, 268*, 4190–4199.
26. Menu-Bouaouiche, L., Vriet, C., Peumans, W. J., Barre, A., Van Damme, E. J., & Rougé, P. (2003). A molecular basis for the endo-beta 1, 3-glucanase activity of the thaumatin-like proteins from edible fruits. *Biochimie, 85*, 123–131.
27. Mani, T., & Manjula, S. (2010). Cloning and characterization of two osmotin isoforms from *Piper colubrinum*. *Biologia Plantarum, 54*, 377–380.
28. Vanaja, T., Neema, V. P., Mammootty, K. P., & Rajeshkumar, R. (2008). Development of a promising interspecific hybrid in black pepper (*Piper nigrum* L.) for *Phytophthora* foot rot resistance. *Euphytica, 161*, 437–445.
29. Hu, X., & Reddy, A. S. N. (1997). Cloning and expression of a PR5-like protein from Arabidopsis: Inhibition of fungal growth by bacterially expressed protein. *Plant Molecular Biology, 349*, 49–59.
30. Bradford, M. M. (1976). A rapid and sensitive method for the quantification of microgram quantities of protein utilizing the principle of protein–dye binding. *Analytical Biochemistry, 723*, 41–74.
31. Broekaert, W. F., Terras, F. R. G., Cammue, B. P. A., & Vanderleyden, J. (1990). An automated quantitative assay for fungal growth inhibition. *FEMS Microbiology Letters, 69*, 55–60.
32. Salzman, R. A., Koiwa, H., Ibeas, J. I., Pardo, J. M., Hasegawa, P. M., & Bressan, R. A. (2004). Inorganic cations mediate plant PR5 protein antifungal activity through fungal *Mnn1*-and *Mnn4*-regulated cell surface glycans. *Molecular Plant-Microbe Interactions, 17*, 780–788.
33. Altschul, S. F., Madden, T. L., Schaffer, A. A., Zhang, J., Zhang, Z., Miller, W., et al. (1997). Gapped BLAST and PSI-BLAST: A new generation of protein database search programs. *Nucleic Acid Research, 25*, 3389–33402.
34. Sali, A., & Blundell, T. L. (1993). Comparative protein modelling by satisfaction of spatial restraints. *Journal of Molecular Biology, 234*, 779–815.
35. Kelley, L. A., Gardner, S. P., & Sutcliffe, M. J. (1996). An automated approach for clustering an ensemble of NMR-derived protein structures into conformationally related subfamilies. *Protein Engineering, 9*, 1063–1065.
36. Sippl, M. J. (1993). Recognition of errors in three-dimensional structures of proteins. *Proteins, 17*, 355–362.
37. Morris, G. M., Goodsell, D. S., Halliday, R. S., Huey, R., Hart, W. E., Belew, R. K., et al. (1998). Automated docking using a Lamarckian genetic algorithm and empirical binding free energy function. *Journal of Computational Chemistry, 19*, 1639–1662.
38. Kouwizjer, M. L. C. E., & Grootenhuis, P. D. J. (1995). Parametrization and application of CHEAT95, an extended atom force field for hydrated oligosaccharides. *Journal of Physical Chemistry, 99*, 13426–13436.
39. Aswati Nair, R., Kiran, A. G., Sivakumar, K. C., & Thomas, G. (2010). Molecular characterization of an oomycete-responsive PR-5 protein gene from *Zingiber zerumbet*. *Plant Molecular Biology Reporter, 28*, 128–135.
40. Chan, Y. W., Tung, W. L., Griffith, M., & Chow, K. C. (1999). Cloning of a cDNA encoding the thaumatin-like protein of winter rye (*Secale cereale* L. Musketeer) and its functional characterisation. *Journal of Experimental Botany, 50*, 627–1628.
41. Thevissen, K., Osborn, R. W., Acland, D. P., & Broekaert, W. F. (1997). Specific, high affinity binding sites for an antifungal plant defensin on *Neurospora crassa* hyphae and microsomal membranes. *Journal of Biological Chemistry, 272*, 32176–32181.
42. Thevissen, K., Osborn, R. W., Acland, D. P., & Broekaert, W. F. (2000). Specific binding sites for an antifungal plant defensin from Dahlia (*Dahlia merckii*) on fungal cells are required for

antifungal activity. *Molecular Plant-Microbe Interactions, 13*, 54–61.
43. Veronese, P., Ruiz, M. T., Coca, M. A., Hernandez-Lopez, A., Lee, H., Ibeas, J. I., et al. (2003). In defense against pathogens both plant sentinels and foot soldiers need to know the enemy. *Plant Physiology, 131*, 1580–1590.
44. Hutchins, K., & Bussey, H. (1983). Cell wall receptor for yeast killer toxin: Involvement of (1–6)-$\beta$-D-glucan. *Journal of Bacteriology, 1549*, 161–169.
45. Bussey, H. (1991). K1 killer toxin, a pore-forming protein from yeast. *Molecular Microbiology, 5*, 2339–23431.